Density Functional Molecular Study on the Full Conformational Space of the *S*-4-(2-Hydroxypropoxy)carbazol Fragment of Carvedilol (1-(9H−Carbazol-4-yloxy)-3-[2-(2-methoxyphenoxy)ethylamino]-2-propanol) in Vacuum and in Different Solvent Media

David R. P. Almeida,*,† Luca F. Pisterzi,† Gregory A. Chass,‡ Ladislaus L. Torday,§ Andras Varro,§ Julius Gy. Papp,§,|| and Imre G. Csizmadia†

Department of Chemistry, Lash Miller Laboratories, 80 St. George Street, University of Toronto, Toronto, Ontario, Canada M5S 3H6, Velocet Communications Inc., 210 Dundas St. West, Suite 810, Toronto, Ontario, Canada M5G 2E8, and Department of Pharmacology and Pharmacotherapy and Division of Cardiovascular Pharmacology (Hungarian Academy of Sciences and Szeged University), Szeged University, Dom ter12, Szeged, Hungary-6701

Received: May 21, 2002; In Final Form: August 2, 2002

Density functional theory (DFT) conformational analysis was carried out on the potential energy hypersurface (PEHS) of the carbazole-containing molecular fragment, *S*-4-(2-hydroxypropoxy)-carbazol, of the chiral cardiovascular drug molecule carvedilol, (1-(9H-carbazol-4-yloxy)-3-[2-(2-methoxyphenoxy)ethylamino]-2-propanol). The PEHS was computed in vacuum, chloroform, ethanol, DMSO, and water at the B3LYP/6-31G(d) level of theory. The carbazole ring system was confirmed to be planar, and the resultant PEHS in vacuum contained 19 converged minima, of which the global minima possessed a conformation with χ_1, χ_2, and χ_3 in the anti position and χ_{10} in the g position. Conformer stability for the *S*-4-(2-hydroxypropoxy)carbazol PEHS was influenced by intramolecular hydrogen bonding. Tomasi PCM reaction-field calculations revealed that the lowest SCF energies, relative conformer energies, and solvation free energies ($\Delta G^{\text{solvation}}$) for the *S*-4-(2-hydroxypropoxy)carbazol PEHS were in protic solvents, ethanol and water, because of the larger hydrogen bond donor values of these solvents, which aid in stabilization of the dipole moment created by the carbazole ring system and the oxygen and nitrogen atoms. However, solvent effects contributed most significantly to the stabilization of *S*-4-(2-hydroxypropoxy)carbazol conformers that contained no internal hydrogen bonding, whereas solvent effects were not as important for conformers that contained intramolecular hydrogen bonding.

1. Introduction

1.1. Biological Background. Carvedilol ($C_{24}H_{26}N_2O_4$) is a cardiovascular drug of proven efficiency in the treatment of mild-to-moderate congestive heart failure (CHF), essential hypertension, angina, and in the improvement of left ventricular function. Carvedilol is a lipophilic autonomic nervous system agent that acts as a multiple-action neurohormonal antagonist by producing nonselective beta blockage (β_1 and β_2) and selective alpha blockage (α_1) while also possessing myocardial-protective antioxidant properties.[1,2]

In dealing with chronic heart failure, angina, and hypertension, beta blockers block the activity of cardiac β-adrenergic receptors (both β_1 and β_2) to noradrenaline (NA), reducing cardiac output and oxygen consumption and therefore the total cardiac workload of the heart.[3,4] Carvedilol provides further positive effects by vasodilation (α_1-adrenergic blockage) at peripheral resistance vessels, which decreases preload and afterload, thereby further reducing cardiac work and wall tensions.[5] The U.S. Data and Safety Monitoring Board stopped, for ethical reasons, the clinical investigations of carvedilol before its completion because of greatly lowered mortality rates.[6,7]

A wide variety of different techniques and studies have indicated that the antioxidant activities of carvedilol reside in the carbazole moiety, which allows carvedilol to protect the myocardium and has an antiproliferative effect on intimal tissue, thereby reducing the major risk factor for stroke by cerebroprotection.[8−11] Carvedilol further provides protection against oxygen-containing free radicals generated during cerebral ischemia and stroke. Carvedilol appears to protect vascular function by scavenging these free radicals and protecting against free-radical-induced endothelial dysfunction. It is these reactive radicals that are implicated in the process of programmed cardiac cell death (apoptosis).[12] Moreover, oxygen-containing free radicals are believed to produce damage to many cellular elements such as lipids (for example, LDL particles), proteins, and nucleic acids. In comparison with other organs of the body, the nervous system may be especially vulnerable to oxygen-containing free radicals. The central nervous system (CNS) has a high rate of oxidative metabolic activity and high concentrations of readily oxidizable substrates. Also stemming from this antioxidant property, carvedilol may also prevent the development of nitrate tolerance in patients receiving continuous nitrate therapy.[7,13,14]

1.2. Chemical Background. Carvedilol, (1-(9H-carbazol-4-yloxy)-3-[2-(2-methoxyphenoxy)ethylamino]-2-propanol), is a chiral drug molecule commercially available as a racemic mixture of both its enantiomers (R[+] and S[−]). However,

* Corresponding author. E-mail: dalmeida@medscape.com.
† University of Toronto.
‡ Velocet Communications Inc.
§ Department of Pharmacology and Pharmacotherapy, Szeged University.
|| Division of Cardiovascular Pharmacology, Hungarian Academy of Sciences and Szeged University.

10.1021/jp021253c CCC: $22.00
Published on Web 09/28/2002

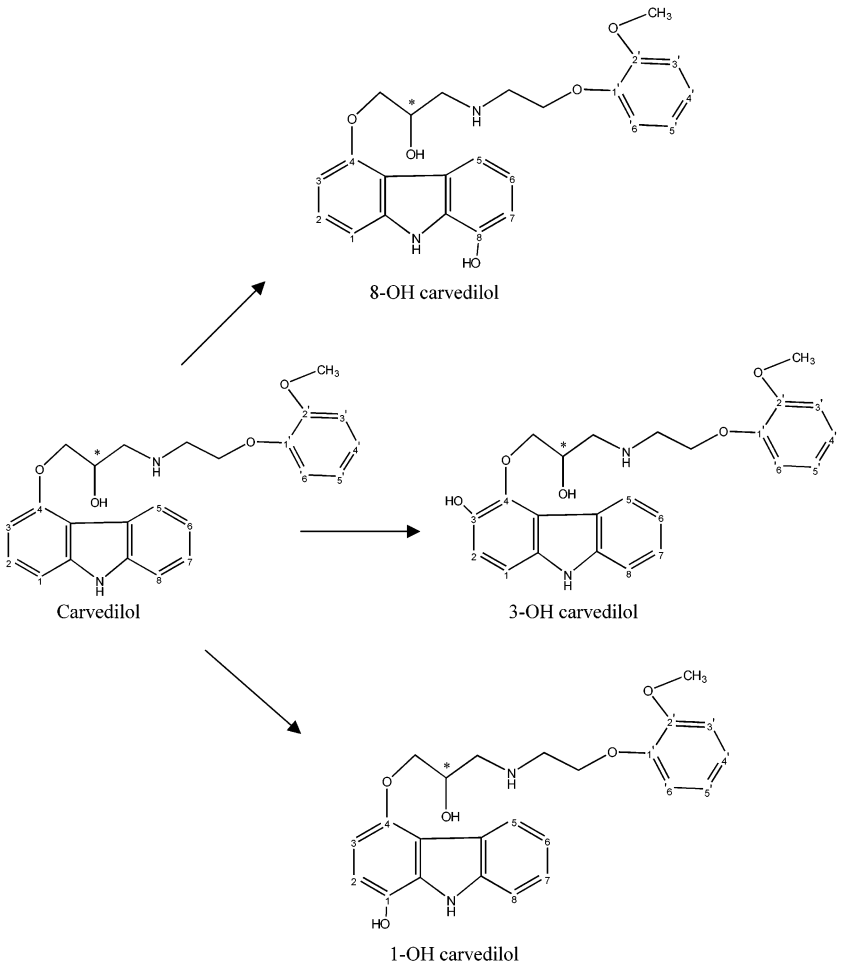

Figure 1. Structure of carvedilol and its antioxidant-marked metabolites. Note that the numbering used is by IUPAC convention (* indicates stereocenter).

the enantiomers of carvedilol show marked stereoselective properties. Both enantiomers have equal α_1 blocking activity and antioxidant activity, but only the S[−] enantiomer contains the nonselective β-adrenergic blocking activity.[10] This represents an unusual situation in which enantiomers of an optically active drug differ not only quantitatively in terms of potency but also qualitatively in that they possess distinct pharmacologic profiles.[15] As such, neither enantiomer alone has the same pharmacologic profile as the racemic mixture of carvedilol used clinically. This phenomena occurs even though the *R*- and *S*-4-(2-hydroxypropoxy)carbazol fragments of carvedilol contain enantiomeric PEHS.

Carvedilol, which is metabolized in the liver, produces antioxidant metabolites devoid of either α_1- or β-adrenergic blocking activity.[16,17] The antioxidant effect is due to the high reaction rates that the carbazole ring undergoes with hydroxyl and peroxide radicals. Carbazole's low redox potential gives carvedilol and its metabolites a powerful tendency to donate electrons more readily in order to "scavenge" the activities of oxygen-containing free radicals (electrons move spontaneously toward oxidant species with more positive redox potentials). However, the striking inhibitory effect of carbazole cannot be explained solely by its radical scavenging ability because its relatively high lipid solubility also provides antioxidant effects against lipid peroxidation.[18] Along with carvedilol, at least one of its three hydroxylated metabolites (cf. Figure 1) is known to have antioxidant properties that inhibit oxidation reactions promoted by the oxygen superoxide ion (O_2^-), hydrogen peroxide (H_2O_2), the hydroxyl radical (•OH), and peroxynitrite ($ONOO^-$) and therefore helps to protect the living body from the deleterious effects of free-radical damage.[19] Carvedilol's metabolites are more effective than vitamin E and in certain experimental setups are more effective than carvedilol itself.[7,12,20,21] The latter is due to the fact that a substitution by a hydroxyl group in a heterocyclic ring such as that of carbazole increases the molecular antioxidant action of that compound.[22]

2. Scope

Carvedilol was divided into three structural fragments according to its chemical activity: *R*- and *S*-4-(2-hydroxypropoxy)carbazol (fragment A) is the antioxidant and β-blocker portion of carvedilol (this analogue structure is similar to β blockers such as propranolol); *R*- and *S*-*N*-ethoxypropane-2-ol (fragment B), which connects the two ether oxygen of carvedilol; and aminoethoxy-2-methoxybenzene (fragment C), which is the chemical structure responsible for the α-blocker action of carvedilol (cf. Figure 2). This chemical fragmentation allows for a progressive study of carvedilol's complete conformational profile.

The objective of this computational study was to analyze the conformational character of *S*-4-(2-hydroxypropoxy)carbazol in different media (cf. Figure 3). A PEHS was first computed in vacuum with a dielectric constant (ϵ) of zero, and the PEHS converged conformers were then evaluated in subsequent protic and aprotic solvent media with higher dielectric constants: chloroform ($CHCl_3$, $\epsilon = 4.9$), ethanol (CH_3CH_2OH, $\epsilon = 24.55$), dimethyl sulfoxide (DMSO, $\epsilon = 46.7$), and water (H_2O, $\epsilon =$

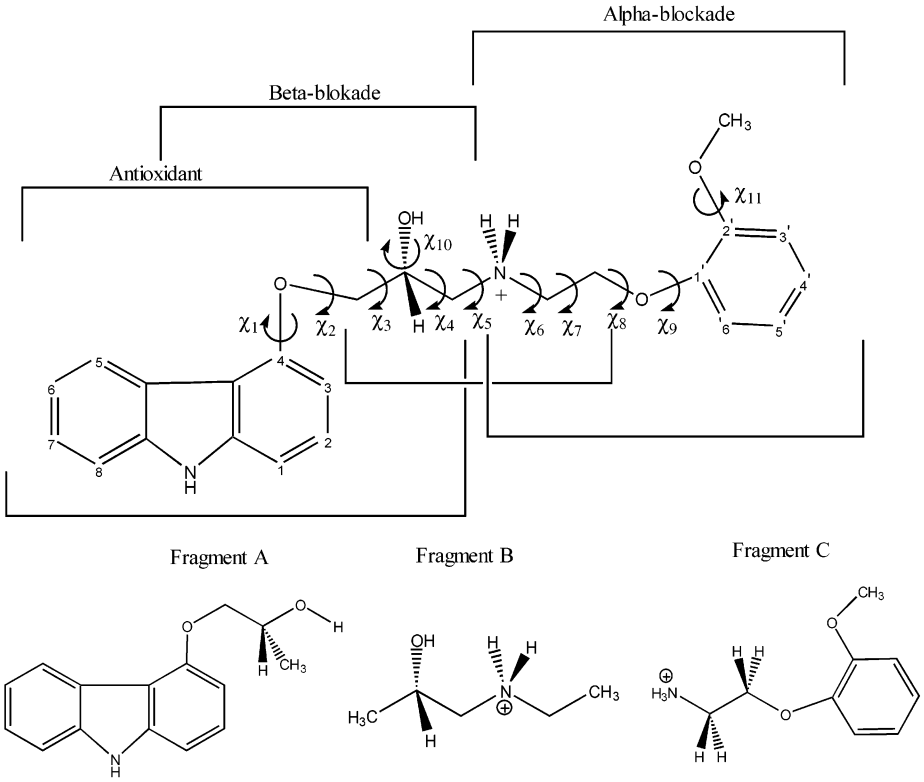

Figure 2. Complete molecular structure and function of *N*-protonated carvedilol indicating all 11 torsional angles (top) and its three characteristic fragments (A, B, and C).

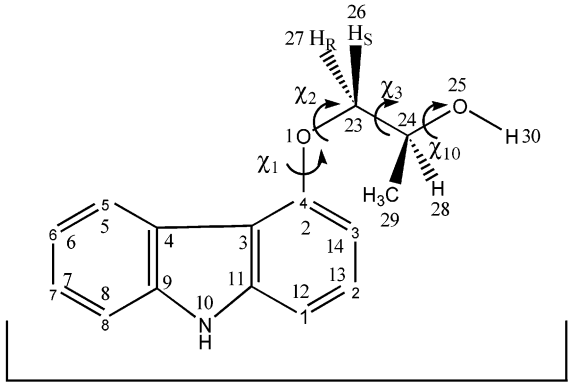

(*S*)-4-(2-hydroxypropoxy)carbazol

$\chi_1 = C^{23}–O^1–C^2\text{-}C^3$ $\chi_3 = C^{29}–C^{24}\text{-}C^{23}\text{-}O^1$

$\chi_2 = C^{24}–C^{23}–O^1\text{-}C^2$ $\chi_{10} = H^{30}\text{-}O^{25}\text{-}C^{24}\text{-}C^{23}$

Figure 3. Numbering and definition of torsional angles for *S*-4-(2-hydroxypropoxy)carbazol. Numbers placed on atoms indicate the IUPAC numbering system, and numbers placed beside atoms indicate the numbering used as *z*-matrix input for Gaussian 98.

78.39). *S*-4-(2-Hydroxypropoxy)carbazol contains a stereocenter (located at C24) with each of the *R*- and *S*-4-(2-hydroxypropoxy)carbazol enantiomers constituting the PEHS with torsional angles χ_1, χ_2, χ_3, and χ_{10} as such:

$$E_S = E_R$$

$$f_S(\chi_1, \chi_2, \chi_3, \chi_{10}) = f_R(-\chi_1, -\chi_2, -\chi_3, -\chi_{10}) \qquad (1)$$

However, only the S enantiomer was studied in this work. Initially, 4-hydroxy carbazol was used to study the orientation of the hydroxyl group as well as the planarity of the carbazole ring structure.

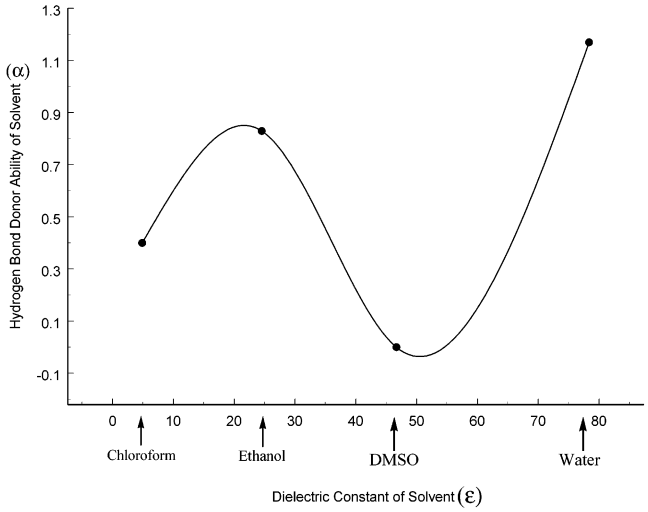

Figure 4. Hydrogen bond donor ability of the solvent (α) as a function of the dielectric constant (ϵ) according to the Abraham−Kamlet−Taff scale for the different solvent media in which the *S*-4-(2-hydroxypropoxy)carbazol was computed.

TABLE 1: Solvent Description According to the Dielectric Constant (ϵ) and Abraham−Kamlet−Taff Scale[a]

solvent	ϵ	π*	α	β
chloroform	4.9	0.58	0.4	0.00
ethanol	24.55	0.54	0.83	0.8
DMSO	46.7	1.00	0.00	0.76
water	78.39	1.09	1.17	0.2

[a] π* describes the index of dipolarity/polarizability, α describes the hydrogen bond donor ability, and β describes the hydrogen bond acceptor ability.[23,24]

Conformations of *S*-4-(2-hydroxypropoxy)carbazol are written in the form $\chi_1[\chi_2\ \chi_3]\chi_{10}$, for example, *g*+[*g*+*g*+]*g*+. Conformations are presented in this manner because of the fact that χ_1

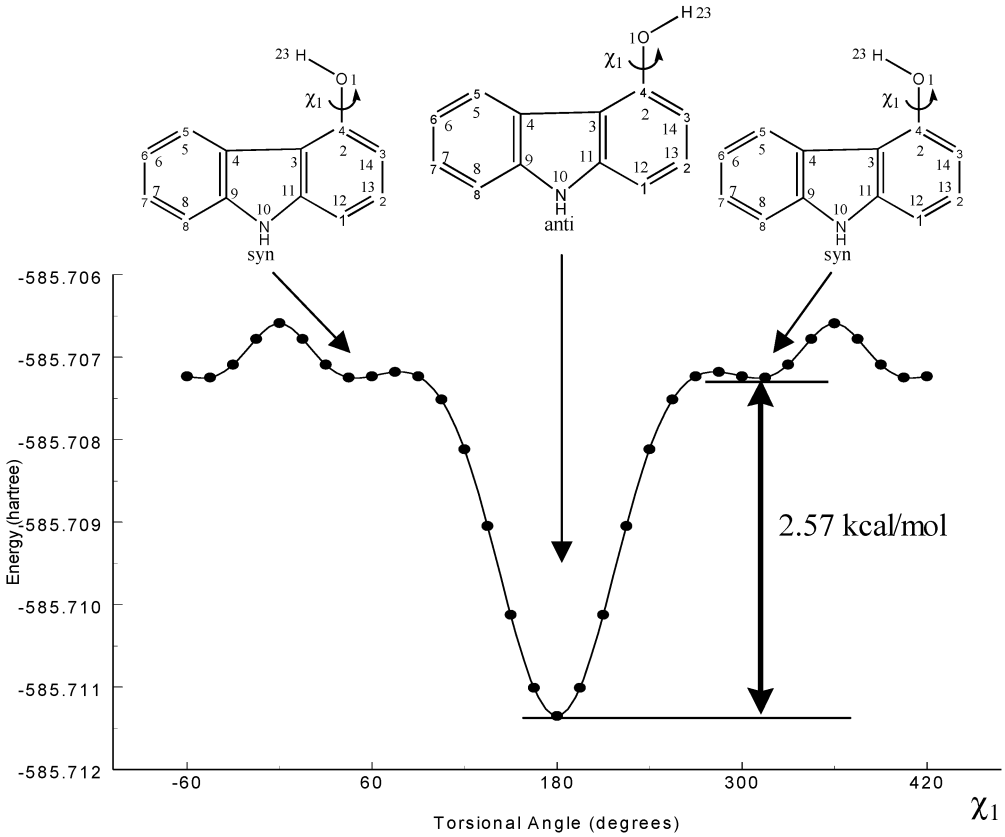

Figure 5. Conformational PEC for torsional angle χ_1 of 4-hydroxycarbazol computed at the RHF/3-21G level of theory.

and χ_{10} represent the torsional angles responsible for the activity of the carvedilol fragment, such as hydrogen bonding, whereas torsional angles χ_2 and χ_3 are responsible for the backbone orientation of *S*-4-(2-hydroxypropoxy)carbazol. Furthermore, each conformer was given a numeric code from 1 to 19, as shown in Table 4, for identification. Torsional angle χ_4, which is associated with the terminal methyl group, was not included because it comprises a symmetrical methyl rotation.

The four different solvents computed can be described according to dielectric constants and the Abraham−Kamlet−Taff scale (cf. Table 1). The Abraham−Kamlet−Taff scale equation (eq 2), first derived by Koppel and Palm, is a multiparametric approach and represents a linear solvation energy relationship (LSER).[23−25]

$$A = A_o + s(\pi^* + d\delta) + a\alpha + b\beta \qquad (2)$$

In the equation, A is the log of the rate or equilibrium constant (A_o is the same as the latter but in the reference solvent cyclohexane), π^* is the index of dipolarity/polarizability (often proportional to the dipole moment), δ is the polarizability correction, α is the hydrogen bond donor ability of the solvent, and β is the hydrogen bond acceptor ability of the solvent.[25]

Of interest to the carvedilol fragment is the ability of the solvent to be a hydrogen bond donor (α). It would be expected that protic solvents with hydrogen bond donor abilities would stabilize *S*-4-(2-hydroxypropoxy)carbazol by hydrogen bonding with the different oxygen and nitrogen atoms of the carvedilol fragment. In Figure 4, the dielectric constant (ϵ) is plotted against the ability of a solvent to be a hydrogen bond donor (α), and the resulting graph shows two peaks indicating the protic solvents ethanol and water, which have significant hydrogen bond donor abilities.

With regards to modeling the environment of *S*-4-(2-hydroxypropoxy)carbazol, one can make the analogy that hydrophobic environments such as cell membranes can be modeled with solvents with low dielectric constants, and hydrophilic environments, with solvents with high dielectric constants. On the basis of the latter, one aprotic (chloroform) and one protic (ethanol) solvent with low dielectric constants were computed along with one aprotic (DMSO) and one protic (water) solvent with high dielectric constants to further differentiate solvent−solute attributes.

3. Computational Method

S-4-(2-Hydroxypropoxy)carbazol was exclusively defined using the Gaussian 98 *z*-matrix internal coordinate system to define molecular structure, stereochemistry, and geometry.[26] Conformational assignments that yielded corresponding minima were selected and evaluated successively at the RHF/3-21G and RHF/6-31G(d) levels of theory (data not shown), and then full optimizations were carried out at the B3LYP/6-31G(d) level of theory in vacuum ($\epsilon = 0.00$). Vibrational frequency calculations were performed on all minima at the B3LYP/6-31G(d) level of theory to ensure that the optimized conformers were true minima and contained no imaginary frequencies. Potential energy curves (PEC) were calculated at the RHF/3-21G level of theory and were plotted using Axum 5.0.

The energies and solvation free energies ($\Delta G^{solvation}$) of the minima were then computed according to the polarized continuum (overlapping spheres) model (PCM) of Tomasi and coworkers with reaction-field calculations in different solvent media at the B3LYP/6-31G(d) level of theory.[27−29] Two aprotic (chloroform, DMSO) and two protic (ethanol, water) solvents were used to span a dielectric solvent range from 4.9 to 78.39 (cf. Scope). $\Delta G^{solvation}$ describes the free energy of dissolving a

TABLE 2: Optimized Minima for 4-Hydroxycarbazol

torsional angle χ_1 RHF/3-21G; B3LYP/6-31G(d) (degrees)	energy RHF/3-21G; B3LYP/6-31G(d) (hartrees)	relative energy RHF/3-21G; B3LYP/6-31G(d) (kcal mol^{-1})
49.95; 11.91	−585.707253023; −592.685596590	2.57; 1.47
−179.99; 180.00	**−585.711349552; −592.687846456**	**0.00; 0.00**
−50.03; −11.91	−585.707252997; −592.685596593	2.57; 1.47

TABLE 3: Summary of Density Functional Conformational PEHS for *S*-4-(2-Hydroxypropoxy)carbazol[a]

conformational assignment					conformational assignment					conformational assignment				
χ_1	χ_2	χ_3	χ_{10}		χ_1	χ_2	χ_3	χ_{10}		χ_1	χ_2	χ_3	χ_{10}	
g^+	g^+	g^+	g^+	**FOUND**	a	g^+	g^+	g^+	NOT FOUND	g^-	g^+	g^+	g^+	NOT FOUND
g^+	g^+	g^+	a	NOT FOUND	a	g^+	g^+	a	NOT FOUND	g^-	g^+	g^+	a	NOT FOUND
g^+	g^+	g^+	g^-	NOT FOUND	a	g^+	g^+	g^-	NOT FOUND	g^-	g^+	g^+	g^-	NOT FOUND
g^+	g^+	a	g^+	NOT FOUND	a	g^+	a	g^+	NOT FOUND	g^-	g^+	a	g^+	NOT FOUND
g^+	g^+	a	a	**FOUND**	a	g^+	a	a	**FOUND**	g^-	g^+	a	a	NOT FOUND
g^+	g^+	a	g^-	**FOUND**	a	g^+	a	g^-	**FOUND**	g^-	g^+	a	g^-	NOT FOUND
g^+	g^+	g^-	g^+	NOT FOUND	a	g^+	g^-	g^+	NOT FOUND	g^-	g^+	g^-	g^+	NOT FOUND
g^+	g^+	g^-	a	NOT FOUND	a	g^+	g^-	a	NOT FOUND	g^-	g^+	g^-	a	NOT FOUND
g^+	g^+	g^-	g^-	NOT FOUND	a	g^+	g^-	g^-	NOT FOUND	g^-	g^+	g^-	g^-	NOT FOUND
g^+	a	g^+	g^+	NOT FOUND	a	a	g^+	g^+	**FOUND**	g^-	a	g^+	g^+	**FOUND**
g^+	a	g^+	a	NOT FOUND	a	a	g^+	a	NOT FOUND	g^-	a	g^+	a	NOT FOUND
g^+	a	g^+	g^-	NOT FOUND	a	a	g^+	g^-	NOT FOUND	g^-	a	g^+	g^-	NOT FOUND
g^+	a	a	g^+	NOT FOUND	a	a	a	g^+	**FOUND**	g^-	a	a	g^+	NOT FOUND
g^+	a	a	a	NOT FOUND	a	a	a	a	NOT FOUND	g^-	a	a	a	NOT FOUND
g^+	a	a	g^-	**FOUND**	a	a	a	g^-	**FOUND**	g^-	a	a	g^-	NOT FOUND
g^+	a	g^-	g^+	NOT FOUND	a	a	g^-	g^+	**FOUND**	g^-	a	g^-	g^+	NOT FOUND
g^+	a	g^-	a	NOT FOUND	a	a	g^-	a	**FOUND**	g^-	a	g^-	a	NOT FOUND
g^+	a	g^-	g^-	NOT FOUND	a	a	g^-	g^-	**FOUND**	g^-	a	g^-	g^-	NOT FOUND
g^+	g^-	g^+	g^+	NOT FOUND	a	g^-	g^+	g^+	NOT FOUND	g^-	g^-	g^+	g^+	NOT FOUND
g^+	g^-	g^+	a	NOT FOUND	a	g^-	g^+	a	NOT FOUND	g^-	g^-	g^+	a	NOT FOUND
g^+	g^-	g^+	g^-	NOT FOUND	a	g^-	g^+	g^-	NOT FOUND	g^-	g^-	g^+	g^-	NOT FOUND
g^+	g^-	a	g^+	NOT FOUND	a	g^-	a	g^+	NOT FOUND	g^-	g^-	a	g^+	NOT FOUND
g^+	g^-	a	a	NOT FOUND	a	g^-	a	a	**FOUND (GM)**	g^-	g^-	a	a	NOT FOUND
g^+	g^-	a	g^-	NOT FOUND	a	g^-	a	g^-	NOT FOUND	g^-	g^-	a	g^-	**FOUND**
g^+	g^-	g^-	g^+	NOT FOUND	a	g^-	g^-	g^+	**FOUND**	g^-	g^-	g^-	g^+	NOT FOUND
g^+	g^-	g^-	a	NOT FOUND	a	g^-	g^-	a	**FOUND**	g^-	g^-	g^-	a	NOT FOUND
g^+	g^-	g^-	g^-	NOT FOUND	a	g^-	g^-	g^-	**FOUND**	g^-	g^-	g^-	g^-	**FOUND**

[a] **GM** = global minima.

TABLE 4: Optimized Minima for the PEHS of *S*-4-(2-Hydroxypropoxy)carbazol at the B3LYP/6-31G(d) Level of Theory in Vacuum (ϵ = 0.00)

conformational assignment										
χ_1	χ_2	χ_3	χ_{10}	code	χ_1	χ_2	χ_3	χ_{10}	E (hartrees)	rel E (kcal mol^{-1})
g^+	g^+	g^+	g^+	1	71.61	86.66	54.09	60.83	−785.829262611	5.82
g^+	a	g^+	a	2	85.32	66.14	179.21	−178.06	−785.827598267	6.86
g^+	g^-	g^+	a	3	86.84	84.20	171.19	−37.39	−785.832802691	3.60
g^+	g^-	a	a	4	83.69	−176.18	173.47	−50.51	−785.836021588	1.58
a	a	g^+	a	5	−177.94	80.97	−172.52	−168.69	−785.831134389	4.64
a	g^-	g^+	a	6	178.67	85.87	174.71	−49.02	−785.836186313	1.47
a	g^+	a	g^+	7	−177.32	176.06	65.92	50.13	−785.837144307	0.87
a	g^+	a	a	8	175.39	177.76	179.89	56.41	−785.833845516	2.94
a	**g^-**	**a**	**a**	**9**	**177.90**	**−174.47**	**178.47**	**−47.42**	**−785.838535810**	**0.00**
a	g^+	a	g^-	10	179.81	178.53	−62.41	75.42	−785.834879306	2.29
a	a	a	g^-	11	179.97	178.34	−65.51	176.80	−785.834840973	2.32
a	g^-	a	g^-	12	178.78	179.25	−66.90	−68.60	−785.834719233	2.40
a	a	g^-	a	13	−155.99	−105.18	−163.31	−167.56	−785.831784652	4.24
a	g^+	g^-	g^-	14	179.26	−81.79	−58.53	74.14	−785.833289249	3.29
a	a	g^-	g^-	15	179.66	−82.57	−62.65	175.70	−785.833158489	3.37
a	g^-	g^-	g^-	16	179.84	−82.40	−61.58	−68.66	−785.832614787	3.72
g^-	g^+	a	g^+	17	−84.52	176.61	68.94	53.44	−785.834927222	2.26
g^-	g^-	g^-	a	18	−74.55	−80.08	−166.17	−58.84	−785.830399507	5.11
g^-	g^-	g^-	g^-	19	−78.61	−85.32	−64.51	−66.57	−785.828425975	6.34

substance from vacuum and is a useful parameter when solvents are compared for a given solute.

4. Results and Discussion

4.1. Structural Analysis of the Carbazole Ring with 4-Hydroxycarbazol. The computational study began with 4-hydroxycarbazol. A PEC of torsional angle χ_1 was generated using the hydroxyl group to model the extending side chain of carvedilol and the orientation of the carbazole ring (cf. Figure 5). The PEC shows a global minimum at the anti orientation and two energetically equal enantiomeric local minima located at gauche$^+$ ($g+$) and gauche$^-$ ($g-$). Subsequent full optimizations at RHF/3-21G and B3LYP/6-31G(d) confirmed the carbazole ring system to be planar (cf. Table 2).

4.2. Conformational Analysis of the *S*-4-(2-Hydroxypropoxy)carbazol PEHS in Vacuum (Gas Phase). The PEHS of *S*-4-(2-hydroxypropoxy)carbazol was analyzed by optimizations of its minima. Conformational structural assignment for the conformational minima was made using the following conditions.

TABLE 5: PCM Energies of the *S*-4-(2-Hydroxypropoxy)carbazol PEHS Converged Minima at the B3LYP/6-31G(d) Level of Theory[a]

conformational assignment				*E* (hartrees) chloroform ($\epsilon = 4.9$)	*E* (hartrees) ethanol ($\epsilon = 24.55$)	*E* (hartrees) DMSO ($\epsilon = 46.7$)	*E* (hartrees) water ($\epsilon = 78.39$)	rel *E* (kcal mol^{-1}) chloroform; ethanol; DMSO; water
χ_1	χ_2	χ_3	χ_{10}					
g$^+$	g$^+$	g$^+$	g$^+$	−785.835452016	−785.847280815	−785.838105591	−785.848539067	5.71; 5.83; 5.75; 5.98
g$^+$	g$^+$	a	a	−785.835761703	−785.852014571	−785.839876218	−785.853562891	5.51; 2.86; 4.64; 2.82
g$^+$	g$^+$	a	g$^-$	−785.838938609	−785.851382704	−785.841626431	−785.852679025	3.52; 3.25; 3.54; 3.38
g$^+$	a	a	g$^-$	−785.841782502	−785.854792831	−785.844096606	−785.856067697	1.73; 1.11; 1.99; 1.25
a	g$^+$	a	a	−785.838922339	−785.854637440	−785.842460640	−785.856169766	3.53; 1.21; 3.02; 1.19
a	g$^+$	a	g$^-$	−785.842289029	−785.855924290	−785.845060186	−785.857127836	1.42; 0.40; 1.39; 0.59
a	a	g$^+$	g$^+$	−785.843247677	−785.855541580	−785.846006567	−785.857035590	0.81; 0.64; 0.79; 0.64
a	a	a	g$^+$	−785.841575633	−785.856360024	−785.845115549	−785.858035710	1.86; 0.13; 1.35; 0.02
a	**a**	**a**	**g$^-$**	**−785.844546250**	**−785.856564633**	**−785.847270577**	**−785.858062768**	**0.00; 0.00; 0.00; 0.00**
a	a	g$^-$	g$^+$	−785.841944548	−785.856262168	−785.845202712	−785.857767055	1.63; 0.19; 1.30; 0.19
a	a	g$^-$	a	−785.841847514	−785.856123578	−785.845024812	−785.857584251	1.69; 0.28; 1.41; 0.30
a	a	g$^-$	g$^-$	−785.842012425	−785.856238960	−785.845348877	−785.857757325	1.59; 0.20; 1.21; 0.19
a	g$^-$	a	a	−785.839191302	−785.853278143	−785.842532301	−785.854769318	3.36; 2.06; 2.97; 2.07
a	g$^-$	g$^-$	g$^+$	−785.840462811	−785.854751815	−785.843765296	−785.856185261	2.56; 1.14; 2.20; 1.18
a	g$^-$	g$^-$	a	−785.840011265	−785.853717388	−785.843115115	−785.855089322	2.85; 1.79; 2.61; 1.87
a	g$^-$	g$^-$	g$^-$	−785.840009467	−785.854576586	−785.843462962	−785.856168143	2.85; 1.25; 2.39; 1.19
g$^-$	a	g$^+$	g$^+$	−785.840819204	−785.853101302	−785.843407391	−785.854221604	2.34; 2.17; 2.42; 2.41
g$^-$	g$^-$	a	g$^-$	−785.836715823	−785.848459667	−785.839403800	−785.849810413	4.91; 5.09; 4.94; 5.18
g$^-$	g$^-$	g$^-$	g$^-$	−785.835724176	−785.849366072	−785.839007643	−785.850726739	5.54; 4.52; 5.19; 4.60

[a] Reaction-field calculations were done in chloroform ($\epsilon = 4.9$), ethanol ($\epsilon = 24.55$), DMSO ($\epsilon = 46.7$), and water ($\epsilon = 78.39$).

TABLE 6: PCM $\Delta G^{solvation}$ of the *S*-4-(2-Hydroxypropoxy)carbazol PEHS Converged Minima at the B3LYP/6-31G(d) Level of Theory in Chloroform, Ethanol, DMSO, and Water

conformational assignment				$\Delta G^{solvation}$ (kcal mol^{-1}) chloroform ($\epsilon = 4.9$)	$\Delta G^{solvation}$ (kcal mol^{-1}) ethanol ($\epsilon = 24.55$)	$\Delta G^{solvation}$ (kcal mol^{-1}) DMSO ($\epsilon = 46.7$)	$\Delta G^{solvation}$ (kcal mol^{-1}) water ($\epsilon = 78.39$)
χ_1	χ_2	χ_3	χ_{10}				
g$^+$	g$^+$	g$^+$	g$^+$	−1.83	−7.67	−3.21	−7.39
g$^+$	**g$^+$**	**a**	**a**	**−3.92**	**−12.51**	**−6.54**	**−12.84**
g$^+$	g$^+$	a	g$^-$	−2.12	−8.44	−3.75	−8.37
g$^+$	a	a	g$^-$	−2.08	−8.73	−3.49	−8.68
a	g$^+$	a	a	−3.73	−12.01	−6.00	−12.27
a	g$^+$	a	g$^-$	−2.67	−9.68	−4.49	−9.77
a	a	g$^+$	g$^+$	−2.53	−8.75	−4.33	−8.98
a	a	a	g$^+$	−3.89	−11.75	−6.20	−11.97
a	a	a	g$^-$	−2.81	−8.81	−4.68	−9.15
a	a	g$^-$	g$^+$	−3.37	−10.79	−5.50	−11.08
a	a	g$^-$	a	−3.35	−10.75	−5.44	−11.01
a	a	g$^-$	g$^-$	−3.59	−10.94	−5.78	−11.24
a	g$^-$	a	a	−3.75	−11.03	−6.02	−11.36
a	g$^-$	g$^-$	g$^+$	−3.11	−10.54	−5.20	−10.69
a	g$^-$	g$^-$	a	−3.00	−10.07	−4.99	−10.22
a	g$^-$	g$^-$	g$^-$	−3.32	−10.91	−5.51	−11.18
g$^-$	a	g$^+$	g$^+$	−2.03	−8.21	−3.57	−8.03
g$^-$	g$^-$	a	g$^-$	−1.91	−7.72	−3.37	−7.52
g$^-$	g$^-$	g$^-$	g$^-$	−3.12	−10.11	−5.13	−10.15

$$\text{gauche plus } (g+) = 60 \text{ (ideal)} \pm 50°$$

$$\text{anti } (a) = 180 \text{ (ideal)} \pm 50°$$

$$\text{gauche minus } (g-) = -60 \text{ (ideal)} \pm 50°$$

This is based on the general observation that if one were to rotate a tetrahedral carbon against another tetrahedral carbon the minima would generally fall within the above ranges. Conformers that were located by geometry optimization were termed **FOUND** and those that could not be located within the above thresholds were termed NOT FOUND (cf. Table 3). Conformations not found usually shifted to the nearest neighboring minima on the PEHS. However, if the nearest minima were also annihilated, as was the case for parts of the PEHS that did not contain stable structures, conformers shifted to a nearby stable geometry. For conformers that were found, fully optimized values are shown in Table 4. The PEHS of the *S*-configuration structure contained one global minima with χ_1, χ_2, and χ_3 in the anti position and χ_{10} in the $g-$ position. All minima contained respective enantiomeric pairs with regards to point and axis chirality (data not shown).

Conformer stability for the *S*-4-(2-hydroxypropoxy)carbazol PEHS was influenced by intramolecular hydrogen bonding between O1 and H30 (defined in Figure 3). Out of the four lowest-energy (i.e., with a relative energy of less than 2 kcal mol^{-1} in vacuum) *S*-4-(2-hydroxypropoxy)carbazol conformers, $g+[aa]g-$, $a[g+a]g-$, $a[ag+]g+$, and $a[aa]g-$, all contained a hydrogen bond between O1 and H30 with distances of 2.202, 2.325, 2.293, and 2.258 Å, respectively (cf. Figure 6). However, this is not to say that hydrogen bonding was not present in any other conformers; $g+[g+g+]g+$ (5.82 kcal mol^{-1}, 2.744 Å hydrogen bond), $g+[g+a]g-$ (3.60 kcal mol^{-1}, 2.189 Å hydrogen bond), $g-[ag+]g+$ (2.26 kcal mol^{-1}, 2.247 Å hydrogen bond), and $g-[g-a]g-$ (5.11 kcal mol^{-1}, 2.756 Å hydrogen bond) all contained hydrogen bonds with varying relative energies. Furthermore, the *S*-4-(2-hydroxypropoxy)-carbazol conformers with torsional angles χ_1 or χ_2 in the anti position were energetically aided by having the side chain extend away from the carbazole ring.

4.3. Analysis of the *S*-4-(2-Hydroxypropoxy)carbazol PEHS in Different Solvent Media. DFT was used to investigate

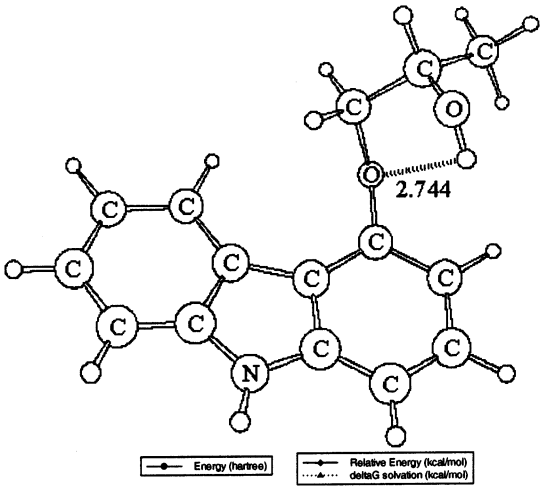

g+[*g*+*g*+]*g*+

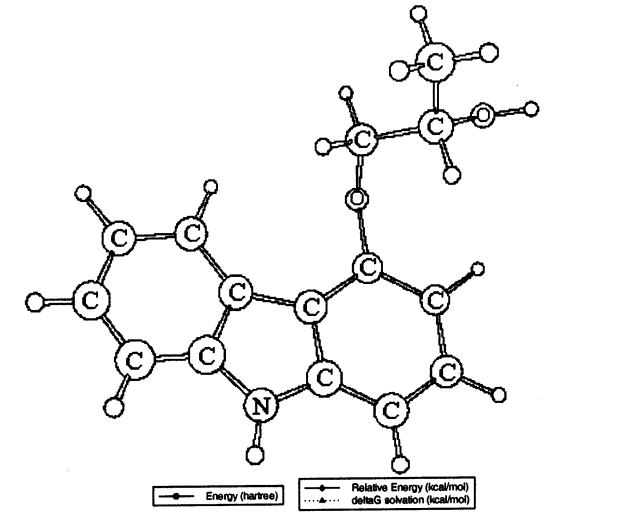

g+[*g*+*a*]*a*

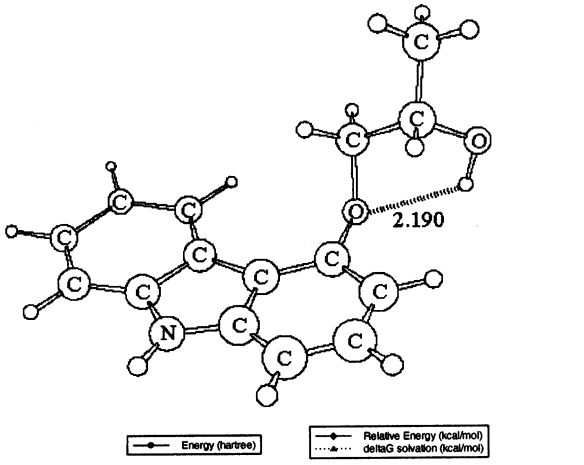

g+[*g*+*a*]g-

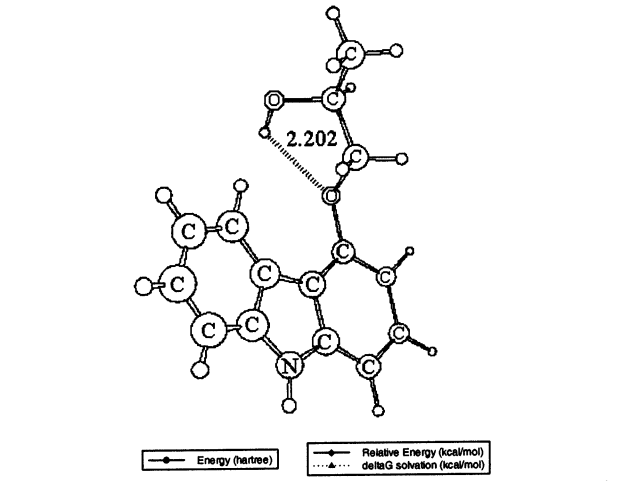

g+[*aa*]g-

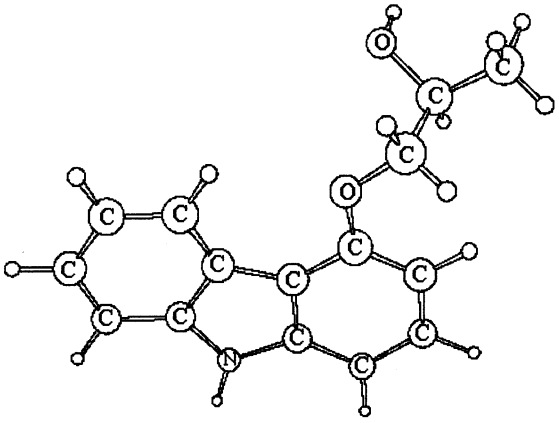

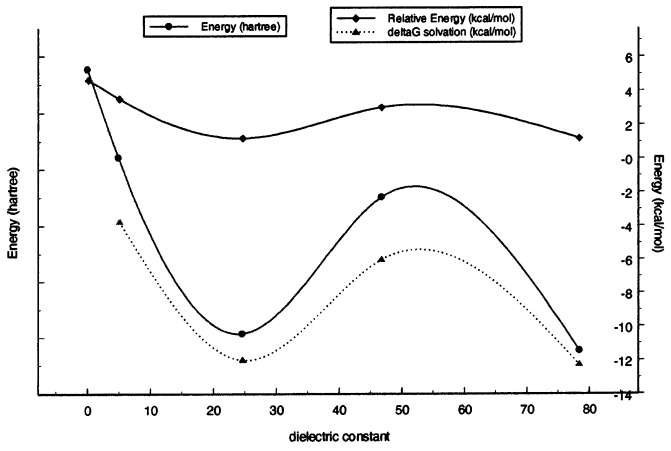

a[*g*+*a*]*a*

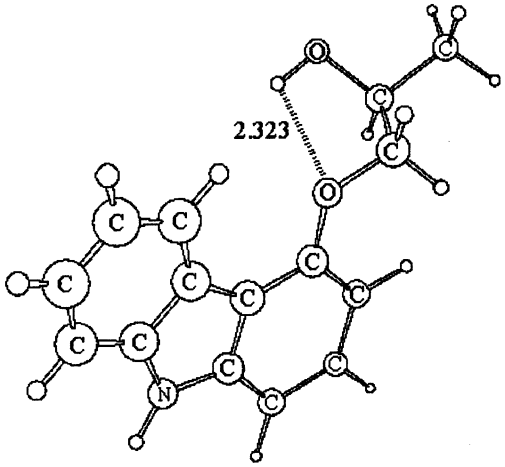

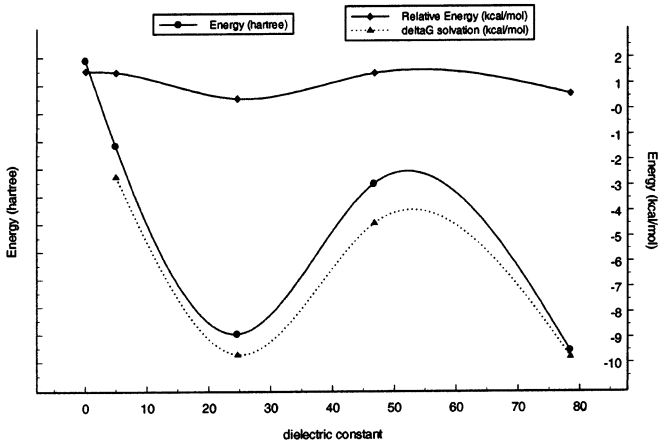

a[*g*+*a*]*g*-

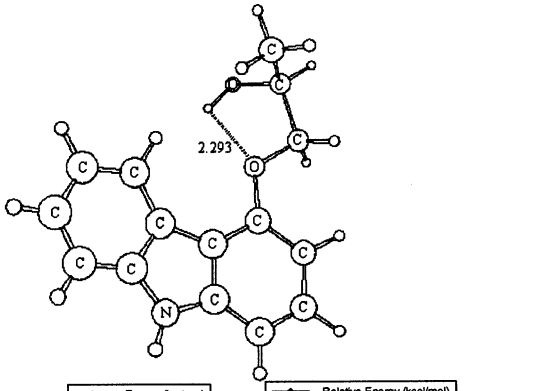

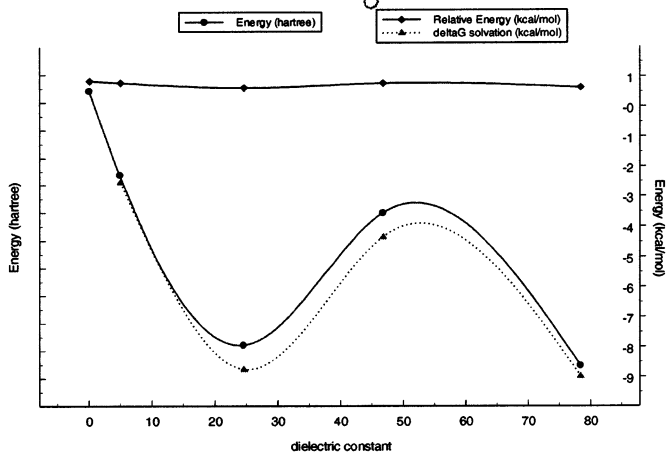

a[*ag*+]*g*+

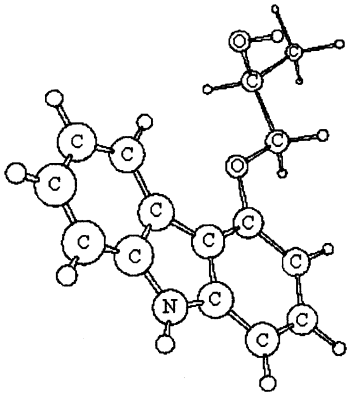

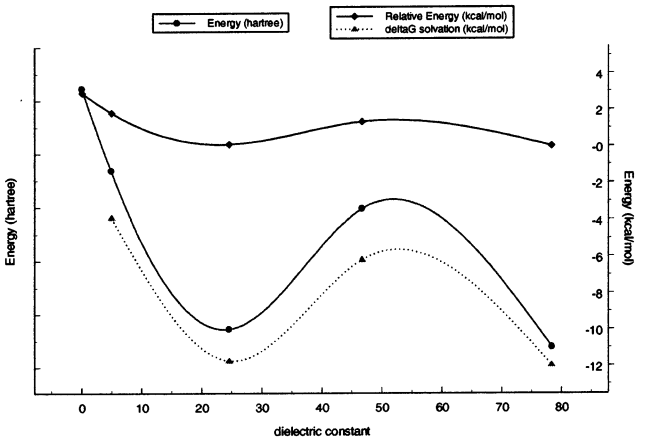

a[*aa*]*g*+

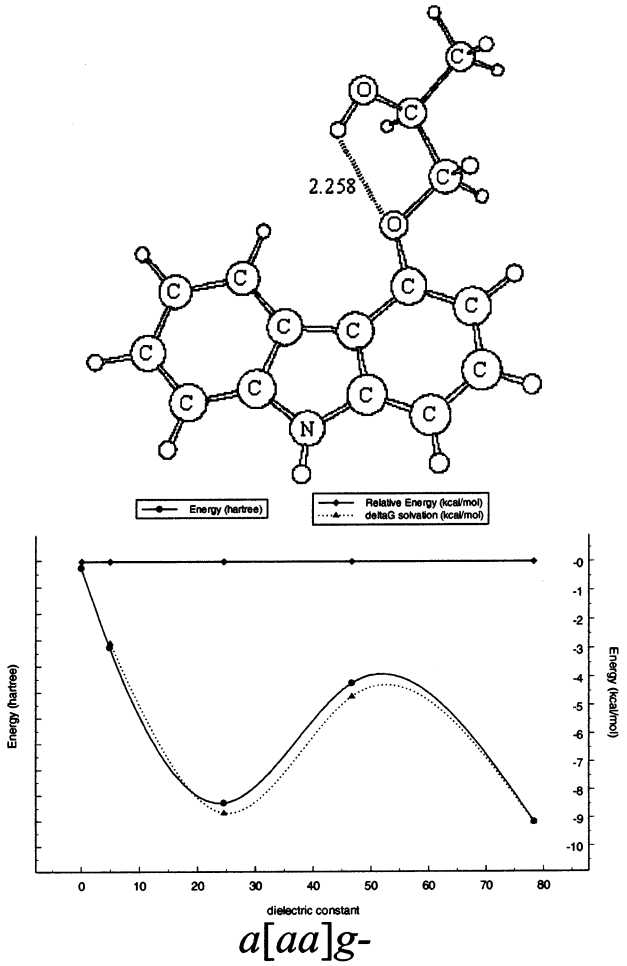

a[*aa*]*g*-

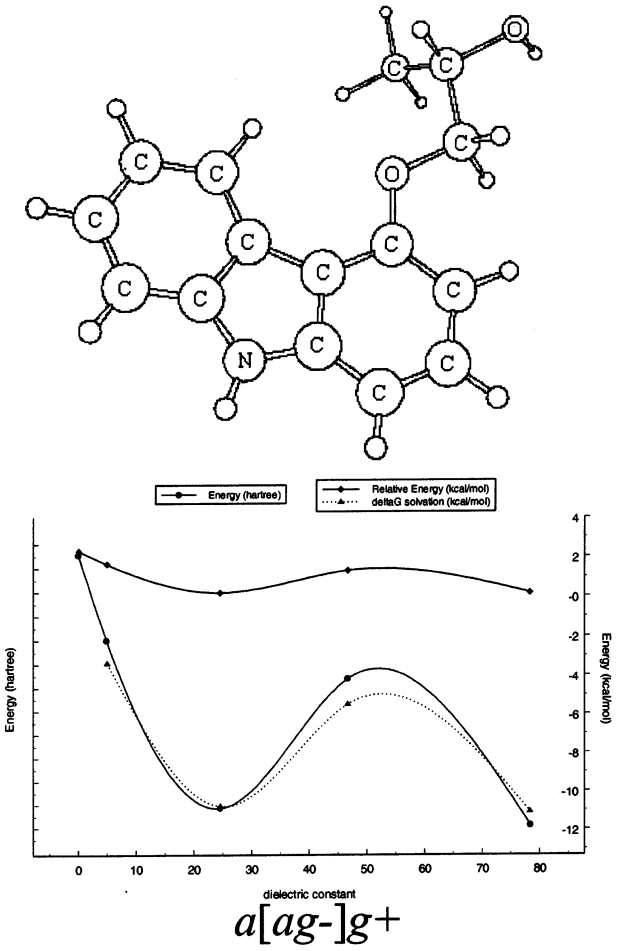

a[*ag*-]*g*+

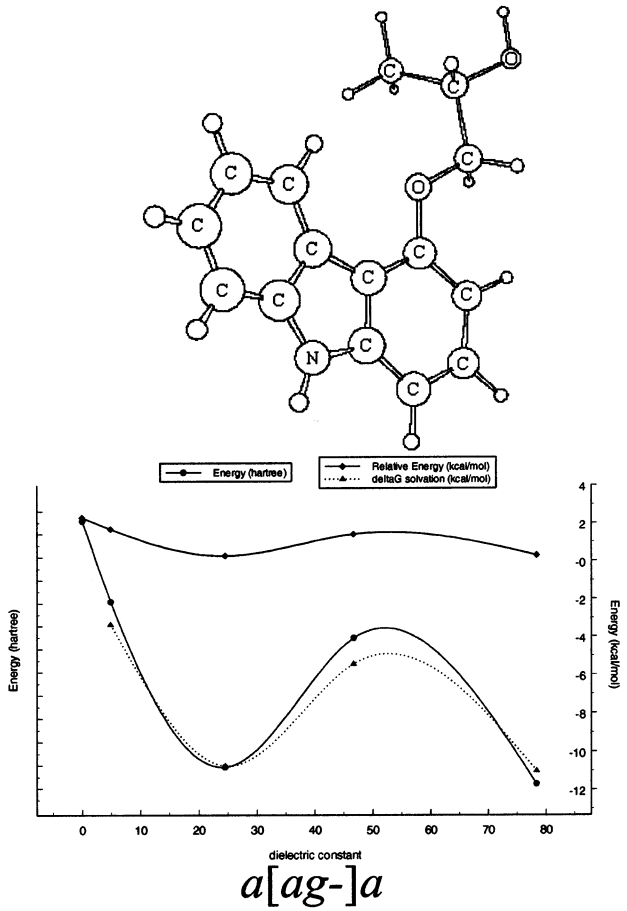

a[*ag*-]*a*

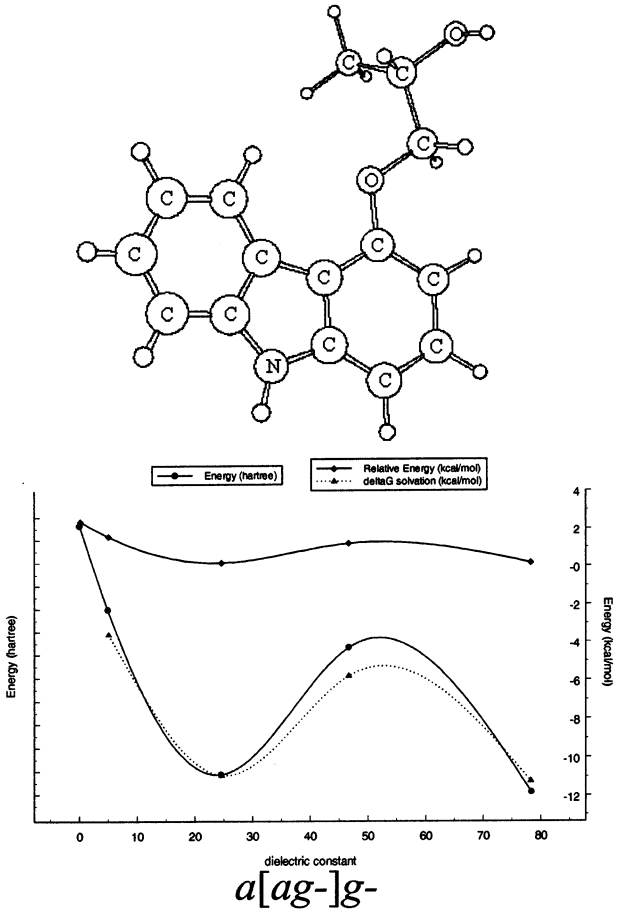

a[*ag*-]*g*-

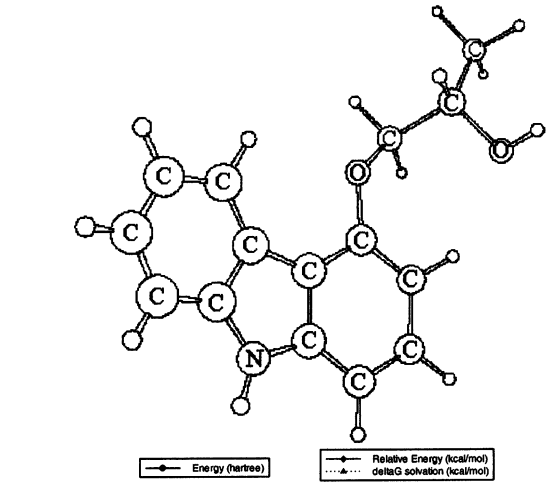

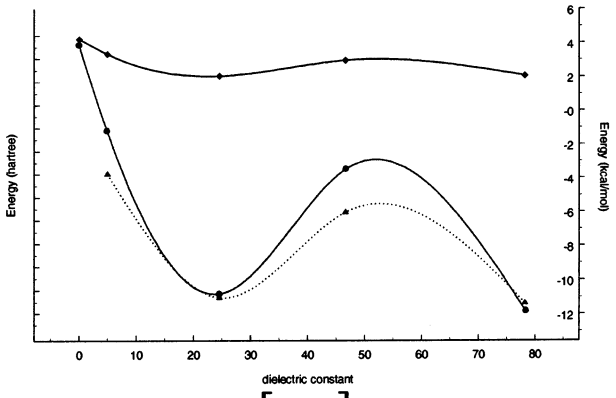

a[*g*-*a*]*a*

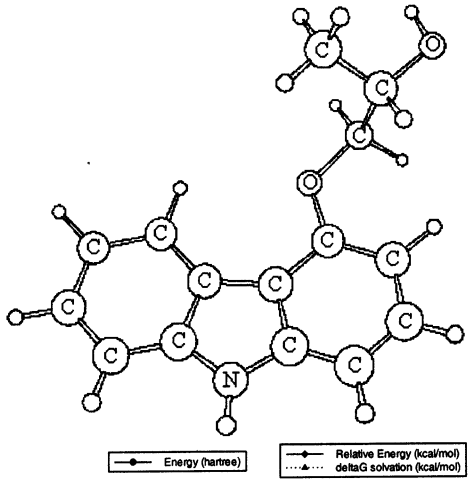

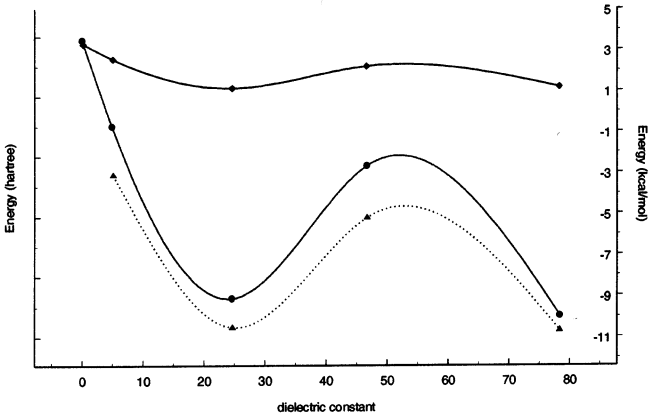

a[*g*-*g*-]*g*+

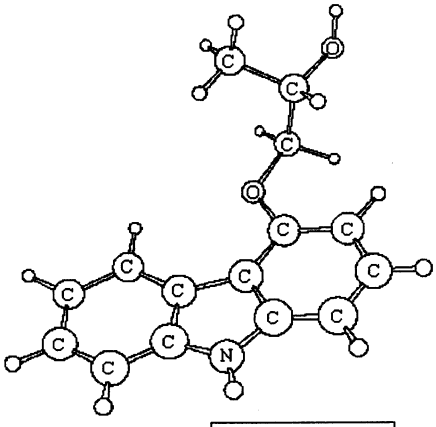

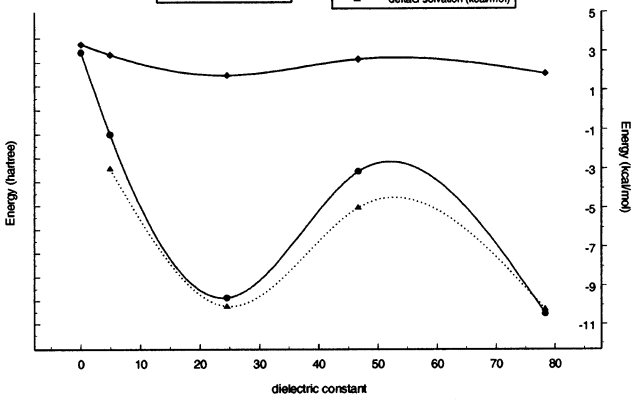

a[*g*-*g*-]*a*

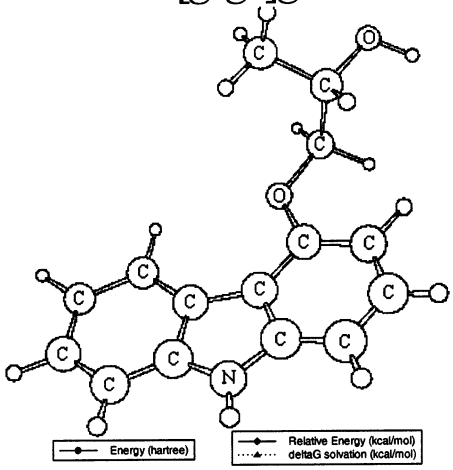

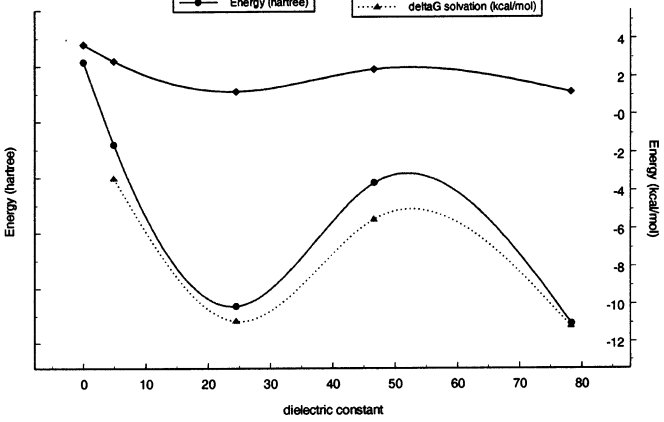

a[*g*-*g*-]*g*-

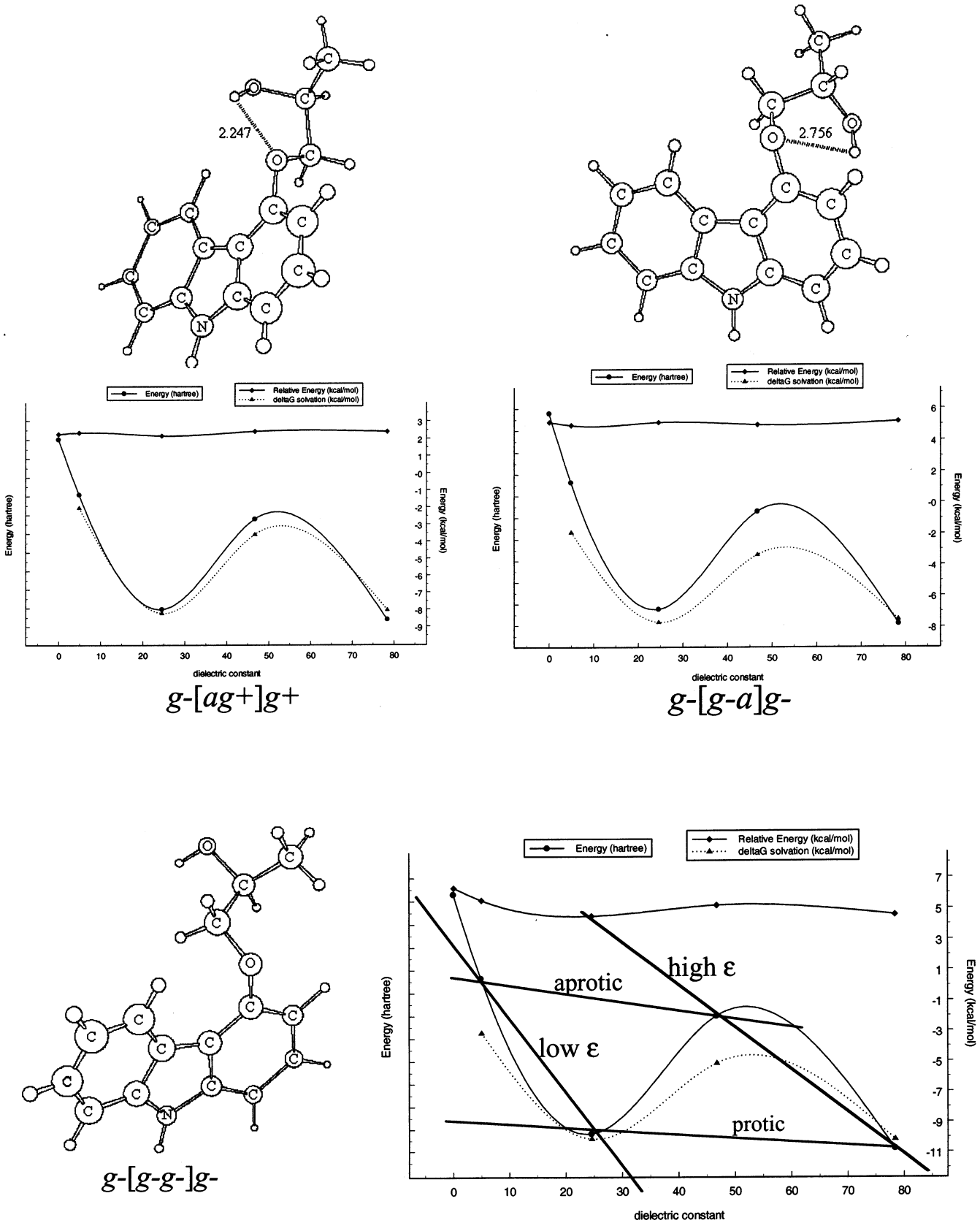

Figure 6. Structures of fully optimized *S*-4-(2-hydroxypropoxy)carbazol PEHS minima at the B3LYP/6-31G(d) level of theory in vacuum. The global conformer is *a*[*aa*]*g*−. Energetic relationships of the *S*-4-(2-hydroxypropoxy)carbazol PEHS converged minima; self-consistent field (SCF) energy (hartrees), relative conformer energy (kcal/mol), and $\Delta G^{\text{solvation}}$ (kcal/mol) as a function of the dielectric constant. Conformer *g*−[*g*−*g*−]*g*− was arbitrarily picked to illustrate the trends of the *S*-4-(2-hydroxypropoxy)carbazol PEHS in different solvent media (cf. Results and Discussion for explanation).

the solute−solvent interactions between *S*-4-(2-hydroxypropoxy)carbazol and various different solvents (chloroform, ethanol, DMSO, water) (cf. Figure 6). The computations were carried out using Tomasi's PCM reaction-field calculations by

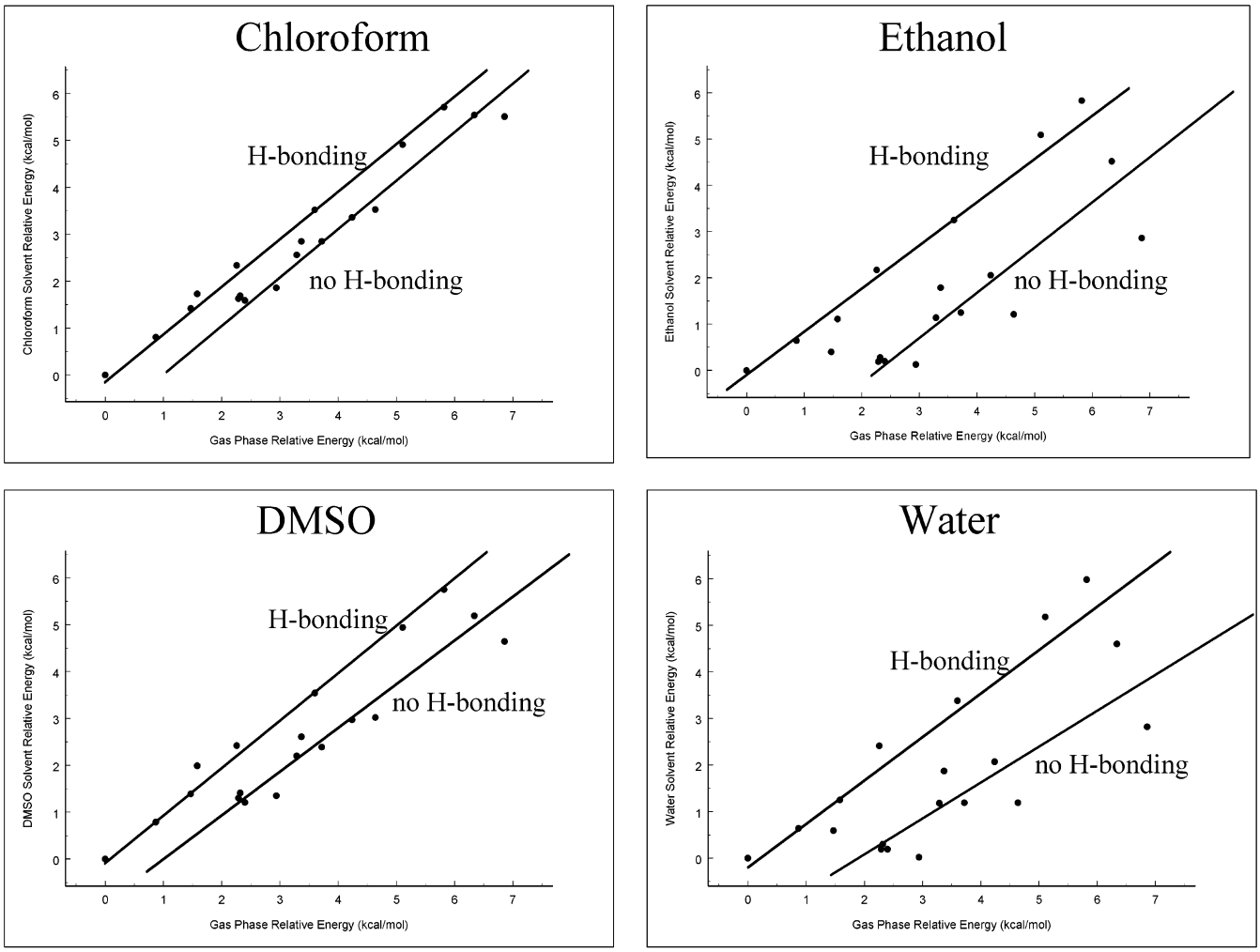

Figure 7. Correlation of relative energies of conformers in solvents with relative energies of conformers in the gas phase.

modeling the reaction field of the various solvents as a continuum of uniform dielectric constant (ϵ) and defining the solute cavity as the union of a series of interlocking atomic spheres.[30]

The trend seen for the *S*-4-(2-hydroxypropoxy)carbazol conformers is that SCF energies, relative energies, and $\Delta G^{\text{solvation}}$ values were all lower (i.e., more negative) in the protic solvents ethanol and water than in the aprotic solvents chloroform and DMSO (cf. Tables 5 and 6). The SCF energy for conformer $g-[g-g-]g-$ was arbitrarily picked to illustrate this trend (cf. last graph in Figure 6). The SCF energy was lower in the protic solvents for both low (ethanol) and high (water) dielectric constant solvents. This can be attributed to the larger hydrogen bond donor values of ethanol and water, which aid in the stabilization of the dipole moment created by the carbazole ring and the oxygen and nitrogen atoms. Moreover, the typical curves generated for SCF energy (hartrees), relative conformer energy (kcal/mol), and $\Delta G^{\text{solvation}}$ (kcal/mol) as a function of dielectric constant all reveal themselves to be similar to an "inverted" version of the curve found in Figure 4. This further emphasizes that the *S*-4-(2-hydroxypropoxy)carbazol conformers, when passing from the gas phase into solution, will be permitted to have the greatest charge separation (electronic polarization) by protic solvents that are able to provide hydrogen bond donor groups.

A further trend observed for all solvents tested is that solvation provides greater stabilization to conformers with no intramolecular hydrogen bonding, as these conformers have structures more accessible to the solvent molecules. *S*-4-(2-Hydroxypropoxy)carbazol conformers with intramolecular hydrogen bonding were stabilized mostly by the inherent hydrogen bonding, and solvation did not play a major role. This is illustrated in Figure 7, showing that conformers with intramolecular hydrogen bonding possess a line similar to $y = x$ of best fit, with a slope of 1. Conformers with no hydrogen bonding possess fitted lines shifted to the right by 1 kcal mol^{-1} in aprotic solvents such as DMSO and about 2 kcal mol^{-1} in protic solvents such as water, indicating greater stabilizing effects by solvation on the relative energies of those conformers with no hydrogen bonding.

Moreover, solvation free energies also correlate with the above trend (cf. Figure 8). The conformers with no internal hydrogen bonding all contained more negative $\Delta G^{\text{solvation}}$ values in all solvents compared with all conformers that possessed internal hydrogen bonding. The conformers with no intramolecular hydrogen bonding had fully extended conformations, enabling them to be fully solvated by the different solvent media, especially the protic solvents. Figure 8 also emphasizes that the effects of solvation on the *S*-4-(2-hydroxypropoxy)carbazol PEHS are similar for a given type of solvent—protic or aprotic—as discerned by the scatter of points. This indicates that conformer stability patterns will not vary widely within the types of either protic or aprotic solvents.

S-4-(2-Hydroxypropoxy)carbazol conformers with no internal hydrogen bonding showed higher relative energies in the gas phase; however, upon solvation with a protic solvent such as

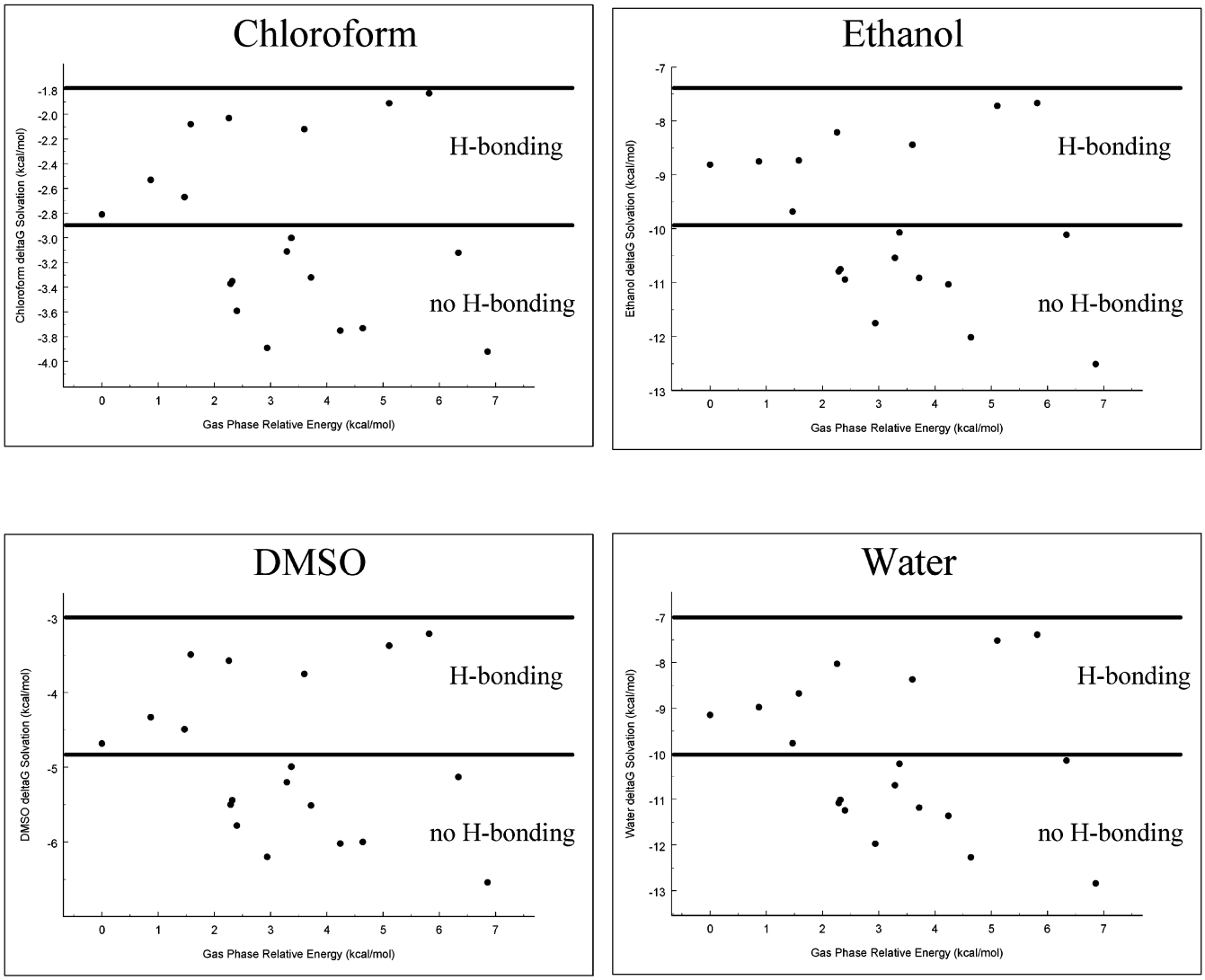

Figure 8. Correlation of $\Delta G^{\text{solvation}}$ of conformers in solvents with relative energies of conformers in the gas phase.

water, their relative energies dropped significantly. An example of the latter is conformer *a*[*aa*]*g*+, which had a relative energy of 2.94 kcal mol^{-1} in the gas phase but upon solvation in water had a solvation relative energy of 0.02 kcal mol^{-1}. This illustrates that internally hydrogen-bonded conformers are not solvated as well as those without hydrogen bonding, and therefore solvent effects are not as important as in cases where no internal hydrogen bonding occurs. Therefore, in molecular systems possessing internal hydrogen bonding, stability is conferred, in majority, by the hydrogen bonding, and these systems are not as influenced by solvent effects, whereas molecular systems with no internal hydrogen bonding will show a greater sensitivity to solvent stabilization effects.

5. Conclusions

For the *S*-4-(2-hydroxypropoxy)carbazol PEHS and, in general, for the two classifications for the media or environment that *S*-4-(2-hydroxypropoxy)carbazol (or another solute) may be in, (i) the environment may be classified as hydrophobic if the dielectric constant is less that 40 (example solvents are chloroform and ethanol) or hydrophilic if the dielectric constant is greater than 40 (example solvents are DMSO and water); and (ii) the media may be aprotic (chloroform and DMSO) or protic (ethanol and water). Resulting solute−solvent properties will be dependent accordingly on the inherent solute chemical properties (for example, stabilization forces) and their respective interactions with the biological environment in question. Finally, possible future work includes modeling the water solvent with explicit water molecules to further look at conformer stability.

References and Notes

(1) Carlson, W.; Oberg, K. *J. Cardiovasc. Pharmacol. Ther.* **1999**, *4*, 205.

(2) Capomolla, S.; Febo, O.; Gnemmi, M.; Riccardi, G.; Opasich, C.; Carporotondi, A.; Mortara, A.; Pinna, G.; Cobelli, F. *Am. Heart J.* **2000**, *139*, 596.

(3) Metra, M.; Nodari, S.; D'Aloia, A.; Bontempi, L.; Boldi, E.; Dei Cas, L. *Am. Heart J.* **2000**, *139*, 511.

(4) Feuerstein, G.; Ruffolo, R. R., Jr. *Adv. Pharmacol. (San Diego)* **1998**, *42*, 611.

(5) Saijonmaa, O.; Metsarinne, K.; Fyhrquist, F. *Blood Pressure* **1997**, *6*, 24.

(6) Packer, M.; Bristow, M. R.; Cohn, J. N.; Colucci, W. S.; Fowler, M. B.; Gilbert, E. M.; Shusterman, N. H. *N. Engl. J. Med.* **1996**, *334*, 1349.

(7) Berg, M. A.; Chasse, G. A.; Deretey, E.; Fuzery, A. K.; Fung, B. M.; Fung, D. Y. K.; Henry-Riyad, H.; Lin, A. C.; Mak, M. L.; Mantas, A.; Patel, M.; Repyakh, I. V.; Staikova, M.; Salpietro, S. J.; Tang, T.-H.; Vank, J. C.; Perczel, A.; Csonka, G. I.; Farkas, O.; Torday, L. L.; Szekely, Z.; Csizmadia, I. G. *J. Mol. Struct.: THEOCHEM* **2000**, *500*, 5.

(8) Hauf-Zachariou, U.; Blackwood, R. A.; Gunawardena, K. A.; O'Donnell, J. G.; Garnham, S.; Pfarr, E. *Eur. J. Clin. Pharmacol.* **1997**, *52*, 95.

(9) Noguchi, N.; Nishino, K.; Niki, E. *Biochem. Pharmacol.* **2000**, *159*, 1069.

(10) Yue, T. L.; Lysko, P. G.; Barone, F. C.; Gu, J. L.; Ruffolo, R. R., Jr.; Feuerstein, G. Z. *Ann. N.Y. Acad. Sci.* **1994**, *738*, 230.

(11) Guazzi, M.; Agostoni, P.; Matturri, M.; Pontone, G.; Guazzi, M. D. *Am. Heart. J.* **1999**, *138*, 460.

(12) Ruffollo, R. R., Jr.; Feuerstein, G. Z. *J. Cardiovasc. Pharmacol.* **1998**, *32* (Suppl. 1), S22.

(13) Yoshioka, T.; Iwamoto, N.; Tsukahara, F.; Irie, K.; Urakawa, I.; Muraki, T. *Br. J. Pharmacol.* **2000**, *129*, 1530.

(14) Watanabe, H.; Karihana, M.; Ohtsuka, S.; Sugishita, Y. *J. Am. Coll. Cardiol.* **1998**, *32*, 1194.

(15) Ruffolo, R. R., Jr.; Gellai, M.; Hieble, J. P.; Willette, R. N.; Nichols, A. J. *Eur. J. Clin. Pharmacol.* **1990**, *38*, S82.

(16) Gehr, T. W.; Tenero, D. M.; Boyle, D. A.; Qian, Y.; Sica, D. A.; Shusterman, N. H. *Eur. J. Clin. Pharmacol.* **1999**, *55*, 269.

(17) van der Does, R.; Hauf-Zachariou, U.; Pfarr, E.; Holtbrugge, W.; Konig, S.; Griffiths, M.; Lahiri, A. *Am. J. Cardiol.* **1999**, *83*, 643.

(18) Searlee, A. J. F.; Gree, C.; Wilson, R. L. Ellipticines and Carbazoles as Antioxidants. In *Oxygen Radicals and Biology*; Borns, W., Saran, M., Tait, D., Eds.; Walter de Gruyter & Co.: Berlin, 1984; pp 377−381.

(19) Feuerstein, G.; Yue, T. L.; Ma, X.; Ruffolo, R. R. *Prog. Cardiovasc. Dis.* **1998**, *41* (Suppl. 1), 17.

(20) Oldham, H. G.; Clarke, S. E. *Drug Metab. Dispos.* **1997**, *25*, 970.

(21) Feuerstein, R.; Yue, T. L. *Pharmacology* **1994**, *48*, 385.

(22) Yue, T. L.; Mckenna, P. J.; Lysko, P. G.; Gu, J. L.; Lysko, K. A.; Ruffolo, R. R., Jr.; Feuerstein, G. Z. *Eur. J. Pharmacol.* **1994**, *251*, 237.

(23) Abboud, J. L.; Kamlet, M. J.; Taft, R. W. *J. Am. Chem. Soc.* **1977**, *99*, 6027. Abboud, J. L.; Kamlet, M. J.; Taft, R. W. *J. Am. Chem. Soc.* **1977**, *99*, 8325.

(24) Abboud, J. L.; Kamlet, M. J.; Taft, R. W. *Prog. Phys. Org. Chem.* **1981**, *13*, 485.

(25) Bagno, A. Overview—Empirical and Thermodynamic Methods. *Solvation and Solvent Effects on Organic Reactivity*; Centro CNR Meccanismi Reazioni Organiche, Dipartimento di Chimica Organica: Padova, Italy, 2002; pp 20−22.

(26) Frisch, M. J.; Trucks, G. W.; Schlegel, H. B.; Scuseria, G. E.; Robb, M. A.; Cheeseman, J. R.; Zakrzewski, V. G.; Montgomery, J. A., Jr.; Stratmann, R. E.; Burant, J. C.; Dapprich, S.; Millam, J. M.; Daniels, A. D.; Kudin, K. N.; Strain, M. C.; Farkas, O.; Tomasi, J.; Barone, V.; Cossi, M.; Cammi, R.; Mennucci, B.; Pomelli, C.; Adamo, C.; Clifford, S.; Ochterski, J.; Petersson, G. A.; Ayala, P. Y.; Cui, Q.; Morokuma, K.; Malick, D. K.; Rabuck, A. D.; Raghavachari, K.; Foresman, J. B.; Cioslowski, J.; Ortiz, J. V.; Stefanov, B. B.; Liu, G.; Liashenko, A.; Piskorz, P.; Komaromi, I.; Gomperts, R.; Martin, R. L.; Fox, D. J.; Keith, T.; Al-Laham, M. A.; Peng, C. Y.; Nanayakkara, A.; Gonzalez, C.; Challacombe, M.; Gill, P. M. W.; Johnson, B. G.; Chen, W.; Wong, M. W.; Andres, J. L.; Head-Gordon, M.; Replogle, E. S.; Pople, J. A. *Gaussian 98*, revision A.9; Gaussian, Inc.: Pittsburgh, PA, 1998.

(27) Miertus, S.; Tomasi, J. *Chem. Phys.* **1982**, *65*, 239.

(28) Miertus, S.; Scrocco, E.; Tomasi, J. *Chem. Phys.* **1981**, *55*, 117.

(29) Cossi, M.; Barone, V.; Cammi, R.; Tomasi, J. *Chem. Phys. Lett.* **1996**, *255*, 327.

(30) Foresman, J. B.; Frish, A. Reaction Field Models of Solvation. *Exploring Chemistry with Electronic Structure Methods*, 2nd ed.; Gaussian Inc.: Pittsburgh, PA, 1996; pp 237−249.